Electronic Absorption, Emission and Two-Photon Absorption Properties of Some Functional 1,3,5-Triphenylbenzenes

Suzy. L. Streatfield,[a,b] Claire Pradels,[a] Alphonsine Ngo Ndimba,[a] Nicolas Richy,[a] Anissa Amar,[c] Abdou Boucekkine,[a],* Marie P. Cifuentes,[b] Mark G. Humphrey,[b],* Olivier Mongin,[a] and Frédéric Paul[a],*

Abstract: We report herein the linear optical properties of some extended 1,3,5-triphenylbenzene derivatives **3-X** (X = NO_2, CN, H, OMe, NMe_2, NPh_2) and briefly discuss the two-photon absorption (2PA) cross-sections determined for the derivatives featuring the most electron-rich substituents, contrasting their 2PA performance with the 2PA values previously gathered for their triphenylisocyanurate analogues (**1-X**). When functionalized by electron-releasing substituents at their periphery, **3-X** derivatives are potent substitutes for **1-X** compounds in NLO applications, especially when maximal transparency is not required in the visible range. Some rationalization of this unexpected outcome is proposed based on DFT calculations.

Introduction

Planar octupolar molecules with a trigonal axis have been the focus of sustained attention for some time due to their second-order nonlinear optical (NLO) properties.[1],[2] However, recently they have attracted even greater interest for their third-order NLO properties because of the very promising societal applications for molecules with large 2PA cross-sections.[3] In this context, we have disclosed the 2PA properties of a series of extended 1,3,5-triazinane-2,4,6-triones (**1-X**; Chart 1), more commonly known as triarylisocyanurates,[4] which turned out to be good two-photon absorbers when peripherally functionalized by donor groups (X = OMe, NMe_2, NPh_2).[5] Interestingly, the 2PA cross-sections of related 1,3,5-triphenylbenzene derivatives containing alkene instead of alkyne linkages, such as **2-NHex$_2$** (407 GM), but featuring alkene instead of alkyne linkages, were shown to possess similar two-photon cross-sections to **1-NMe$_2$** (360 GM) and **1-NPh$_2$** (410 GM).[6] This was unexpected, because the central ring in the **1-X** derivatives is more electron-deficient than that in the **2-X** compounds; the increased polarization of the peripheral arms in **1-X** would be expected to enhance 2PA,[3b, 7] although the electronic effect[8] of this structural change is difficult to deconvolute from the planarizing influence of an alkenyl bridge instead of an alkynyl one in **2-NHex$_2$**.[9] To better understand the role of this spacer, we now report the 2PA properties of six functional analogues of **2-NHex** featuring an alkynyl bridge (**3-X**; X = NO_2, CN, H, OMe, NMe_2, NPh_2), a series of 1,3,5-triarylbenzene derivatives that is simultaneously closely related to the **1-X** derivatives and that should therefore provide a useful comparison. This study is complemented by DFT and TD-DFT calculations to afford additional insight into the electronic structure changes arising from the change of the central ring on proceeding from **1-X** to **3-X**.

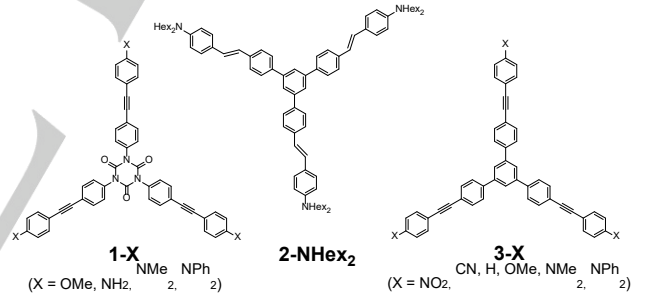

Chart 1. Molecular Structures of the Previously Reported and Targeted Compounds from the Present Work.

Results

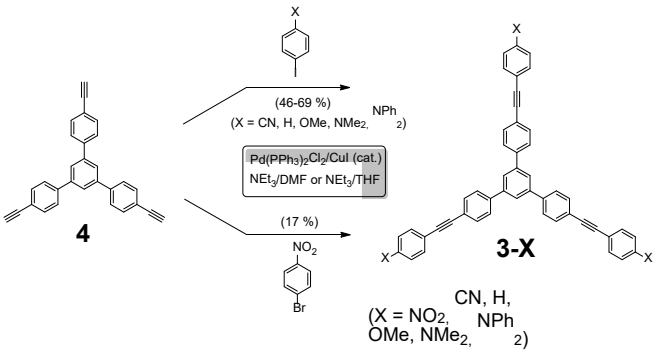

Scheme 1. Synthesis of **3-X**.

[a] S. L. Streatfield, C. Pradels, A. Ngo Ndimba, N. Richy, Prof. A. Boucekkine, Dr. O. Mongin, Dr. F. Paul
Institut des Sciences Chimiques de Rennes, CNRS (UMR 6226)
Université de Rennes 1
Campus de Beaulieu, 35042 Rennes Cedex (France)
Tel: (+33) 02-23-23-59-62
E-mail: frederic.paul@univ-rennes1.fr

[b] S. Streatfield, Prof. M. P. Cifuentes, Prof. M. G. Humphrey
Research School of Chemistry, Australian National University
Canberra, ACT 2601 (Australia)
Tel: (+61) 2-61252927
E-mail: mark.humphrey@anu.edu.au

[c] Dr A. Amar,
Département de Chimie, Faculté des Sciences
Université Mouloud Mammeri
15000 Tizi-Ouzou (Algeria)

Supporting information for this article is given via a link at the end of the document.

Synthesis and Characterization. The targeted compounds were obtained by Sonogashira coupling of the known 1,3,5-tri(4-ethynylphenyl)benzene **4** and the corresponding functional 4-iodobenzenes or 4-bromobenzenes (Scheme 1). In the case of **3-NO₂**, the isolated yield was lower because of purification problems. Two derivatives were known (CN, OMe),[10] but all others are new and were characterized by the usual means.

One- and Two-photon Absorption and Emission Studies. The UV-visible absorption spectra of these extended triphenylbenzenes were recorded. As for the related **1-X** molecules, the **3-X** compounds possess good transparency in the visible range, with a lowest-energy absorption below 400 nm (Table 1), giving yellow solutions. Upon progressing from **3-H** to **3-NPh₂** (corresponding to an increase in the electron-releasing nature of the *para*-substituents), a bathochromic shift of the first absorption is observed, but this is also seen when the *para*-substituents become more electron-withdrawing in nature (Figure 2). This is consistent with the central phenyl ring behaving as an acceptor or as a donor, depending on the nature of the terminal X-substituent. This lowest-energy absorption is much more intense for **3-X** than for **1-X**. A higher-energy absorption (at ca. 290-300 nm) is observed for the **3-X** derivatives with their lowest-energy absorptions at > 350 nm.

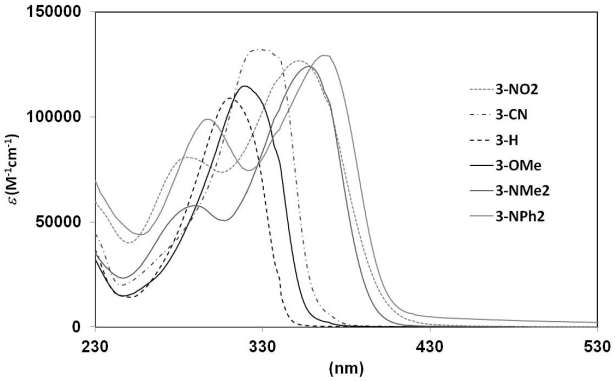

Figure 2. UV-vis spectra for **3-X** (X = NO_2, CN, H, OMe, NMe_2, NPh_2) in CH_2Cl_2 (20 °C).

Table 1. Absorption and emission properties of selected cyclotrimers **1-X** and **3-X** in dichloromethane at 25 °C.

Cmpd	λ_{abs} (nm)	$10^{-3}\,\varepsilon_{max}$ ($M^{-1}.cm^{-1}$)	λ_{em} (nm)	Φ [a]	Stokes shift [b] (cm^{-1})	DFT: λ_{max} (nm) [*f*][c] in CH_2Cl_2 CAM-B3LYP/6-31*G[d]	DFT: λ_{max} (nm) [*f*][c] in CH_2Cl_2 B3LYP/6-31*G[d][5b]
1-CN[11]	317	98.7	333	0.58	1516	306 [2.40]	/
						306 [2.42]	
	300	100.7				250 [0.05]	
1-OMe	316	106.4	348	0.025	4600	299 [2.30]	333 [2.03]
						299 [2.0]	
	264	44.4	/	/	/	248 [0.04]	247 [0.12]
1-NMe_2	352	109.6	418	0.200	4500	337 [2.54]	375 [2.00]
						337 [2.60]	
	288	34.1	/	/	/	269 [0.11]	266 [0.49]
1-NPh_2	364	99.0	437	0.730	4600	340 [2.50]	404 [1.95]
						340 [2.52]	
	294	56.4	/	/	/	270 [0.53]	298 [0.80]
3-NO_2	352	126.8	457	0.005	6500	345 [2.60]	/
						345 [2.60]	
	285	80.7	/	/	/	262 [0.18]	
3-CN	328	132.0	375	0.62	3800	324 [2.95]	/
						323 [2.94]	
	n.o.[e]	/	/	/	/	250 [0.01]	
3-H	310	109.0	364	0.50	4800	306 [2.65]	/
						306 [2.64]	
	n.o.[e]	/	/	/	/	222 [0.04]	
3-OMe	319	114.8	375	0.73	4700	315 [2.91]	/
						315 [2.88]	
	n.o.[e]	/	/	/	/	248 [0.03]	
3-NMe_2	357	124.1	454	0.69	6000	334 [3.05]	/
						334 [3.06]	
	290	57.5	/	/	/	266 [0.06]	
3-NPh_2	366	129.0	450	0.73	5100	346 [3.12]	/
						346 [3.12]	
	297	98.8	/	/	/	271 [0.75]	

[a] Fluorescence quantum yield in CH_2Cl_2 when excited at λ_{abs} (Standard: quinine bisulfate in 0.5 M H_2SO_4). [b] Stokes shift = $(1/\lambda_{abs} - 1/\lambda_{em})$. [c] *f* = oscillator strength. [d] Functionals used. [e] n.o. = not observed in CH_2Cl_2.

All the new cyclotrimers **3-X** are luminescent in solution (Table 1). With the exception of the nitro derivative **3-NO$_2$**, luminescence appears to increase with the increasing electron-releasing or electron-withdrawing power of the substituent and is maximized (73 %) for the diphenylamino derivative **3-NPh$_2$**. When compared to their isocyanurate analogues **1-X** featuring electron-releasing substituents, these compounds appear overall more luminescent (see ESI). Mirror images between the absorption and emission profiles (see Supporting Information) indicate that the strongly absorbing states are also the emitting state for the **3-X** derivatives, while the shoulders observed on the low-energy side of some bands most likely correspond to non-emissive states.

Solvatochromic studies of **3-CN** and **3-NPh$_2$** reveal that emission is much more solvent-sensitive than absorption, regardless of the nature of the terminal substituent, with a shift to lower energy observed on proceeding to the most polar solvent that follows a Lippert–Mataga relationship.[12] The dependency of the Stokes shift on the polarity–polarizability parameter Δf (see ESI) observed for **3-NPh$_2$** is similar to that previously reported for **1-NPh$_2$**.[5b] While qualitatively similar, the solvatochromic dependency of compounds with electron-withdrawing substituents such as **3-CN** are a factor of three less. In both cases, these results are consistent with localization of the (more polar) excited state in one arm of the compound.[13]

Table 2. 2PA properties of selected cyclotrimers in dichloromethane at 25 °C.

Cmpd	λ_{1PA} [a] (nm)	λ_{2PA} [b] (nm)	σ_2 [c] (GM)	σ_2/MW [d] (GM/g)	$\phi.\sigma_2$ [e] (GM)
3-CN	328	≤700	≥75	≥0.11	>46
[f]		640	200	0.293	124
3-OMe	319	≤700	≥36	≥0.05	>26
[f]		640	90	0.129	65
3-NMe$_2$	357	730	380	0.517	262
3-NPh$_2$	369	760	390	0.352	285
1-NMe$_2$	352	720	360	0.458	72
1-NPh$_2$	364	740	410	0.354	300

[a] Wavelength of the one-photon absorption maximum. [b] Wavelength of the two-photon absorption maximum. [c] TPA cross section at λ_{2PA}. [d] Figure-of-merit relevant for applications in optical limiting or nanofabrication.[14] [e] Two-photon brightness figure-of-merit for imaging applications.[14] In these expressions, ϕ represents the luminescence quantum yield and *MW* the molecular weight. [f] 1PA-extrapolated values from TPEF plot.

The 2PA cross sections were assessed in the near-IR (NIR) range (λ = 700–1000 nm) through investigation of the two-photon excited fluorescence (TPEF). The excitation was performed with femtosecond pulses from a Ti:sapphire laser (Figure 3 and Table 2). Due to instrumental limitations (1PA below 350 nm) or weak luminescence, no TPEF could be detected for **1-H** and **1-NO$_2$**, whereas the **3-X** compounds exhibited sufficient TPEF in the NIR range to allow accurate determination of their 2PA cross-sections. Although only the red edge of the 2PA band could be observed for **3-CN** and **3-OMe**, the maxima for the amino derivatives **3-NMe$_2$** and **3-NPh$_2$** were located at λ = 740 nm and 760 nm, respectively, with maximal values of the 2PA cross-sections up to 390 GM). Comparison of these 2PA bands with their 1PA bands reveals that the 2PA maxima are situated close to twice that of the 1PA maxima detected at the lowest energy in the UV range, suggesting that the excited states at the origin of 2PA in the NIR are also active for 1PA (see ESI).

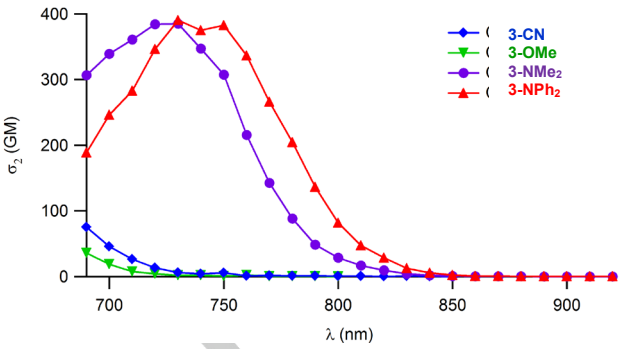

Figure 3. Two-photon absorption spectra for **3-X** (X = CN, OMe, NMe_2, NPh_2) in dichloromethane (20 °C).

DFT Calculations. Density functional theory (DFT) calculations were performed on the **3-X** derivatives (X = NO_2, CN, H, OMe, NMe_2, NPh_2). In these compounds, the three peripheral arms adopt a tilted conformation relative to the central phenyl plane upon geometry optimization in CH_2Cl_2. After optimization, the calculated dihedral angles between the three peripheral arms and the central phenyl plane are in the range 36-37°, slightly less pronounced than the dihedral angles of the **1-X** analogues (55°-80°).[5b]

The HOMO-LUMO gap in these derivatives (Table 3) is smaller than that in the corresponding isocyanurate analogues (**1-X**). Starting from **3-H**, the calculations reveal that this gap progressively decreases when increasingly electron-withdrawing or electron-releasing substituents are installed on the periphery, mirroring the trend in energies seen experimentally for the lowest-lying intense absorptions of these compounds (Table 1). TD-DFT calculations reproduce fairly well the most intense transitions at lowest energy (Table 1) and confirm the observed increase in oscillator strength on proceeding from **1-X** to **3-X**. Experimental observations are most accurately reproduced using the CAM-B3LYP functional. Although they are somewhat underestimated in all cases,[15] the computed longest wavelengths are within 2000 cm^{-1} of the experimental data for the **3-X** derivatives with this functional.

Similar to calculations on the **1-X** compounds,[5b] the TD-DFT computations on the **3-X** derivatives confirm that the strong transitions correspond to multiconfigurational excitations. Depending on the functional used (see ESI), the nature of the underlying excitations changes slightly within the HOMO/HOMO-2 and LUMO+2/LUMO manifolds which each constitute a pair of nearly degenerate frontier MOs (of E and A symmetry, respectively, for strict C_{3v} geometry). Thus, the lowest-energy transition corresponds to a symmetrical charge transfer between the periphery and the center, with a dominant $\pi^* \leftarrow \pi$ character ($E \leftarrow A$ under strict C_3 symmetry). Consistent with the ambivalent acceptor/donor character of the central ring, the charge transfer occurs from the periphery towards the centre when X is electron-releasing or in the reverse direction when X is electron-

withdrawing, analogous to the lowest-energy transition observed with the **1-X** analogues.[5b, 11] The intense absorption at higher energy, only observed in the present system for compounds with the most electron-withdrawing or –releasing substituents **3-NO$_2$**, **3-NMe$_2$**, and **3-NPh$_2$**, also corresponds to an allowed π-π* transition, but involves deeper lying occupied MOs (see ESI), and as a result, this transition is more arm-centered in **3-NPh$_2$**.

Table 3: CAM-B3LYP/6-31G* calculated HOMO-LUMO energy gaps in CH_2Cl_2 for **1-X** and **3-X**.

X	HOMO-LUMO gap (eV)	
	3-X	**1-X**
NO$_2$	5.62	/
CN	6.09	6.45
H	6.42	/
OMe	6.23	6.30
NMe$_2$	5.81	5.86
NPh$_2$	5.70	5.82

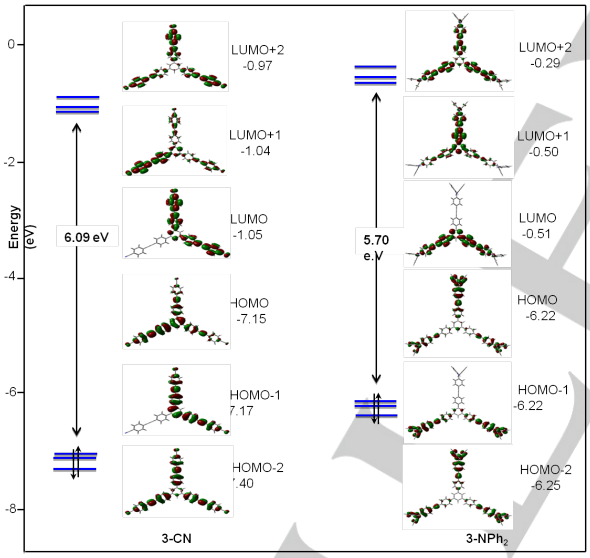

Figure 4. Frontier molecular orbitals involved in the lowest-energy (intense) allowed transition for **3-CN** (a) and **4-NPh$_2$** (b) (isocontour 0.03 [e/bohr3]½).

Discussion

Our investigations clearly demonstrate that the lowest-energy allowed electronic transitions of the **3-X** compounds strongly resemble those of their previously reported **1-X** analogues.[5b] In line with previous studies on related derivatives,[2b] localization of the excited state on one branch in the first excited state is strongly suggested by solvatochromic studies.[13d] Despite these electronic similarities, it appears that the **3-X** compounds are overall more fluorescent than their **1-X** counterparts, especially for examples with less electron-releasing substituents (X = OMe, CN). Thus, in line with expectations based on the Strickler-Berg relationship,[16] the much stronger transition moments for the lowest-energy 1PA absorptions of **3-X** translate to larger emission quantum yields, a feature particularly pronounced for the compounds bearing the less electron-releasing substituents. Alternatively, the increased fluorescence of compounds **3-X** with a central 1,3,5-phenylene core relative to their **1-X** analogues might also be attributed to the absence of low-lying π*←n states able to quench the fluorescence.[5b] Good fluorescence yields are frequently observed for extended star-shaped compounds of this kind.[17] The fluorescence quantum yields found for several of the **3-NR$_2$** derivatives (Table 1) are significantly better than those of the **2-NHex$_2$** analogues in $CHCl_3$ (29%; Chart 1),[2b] suggesting that replacement of the double bonds in the latter by triple bonds with the present series of compounds is beneficial to luminescence.

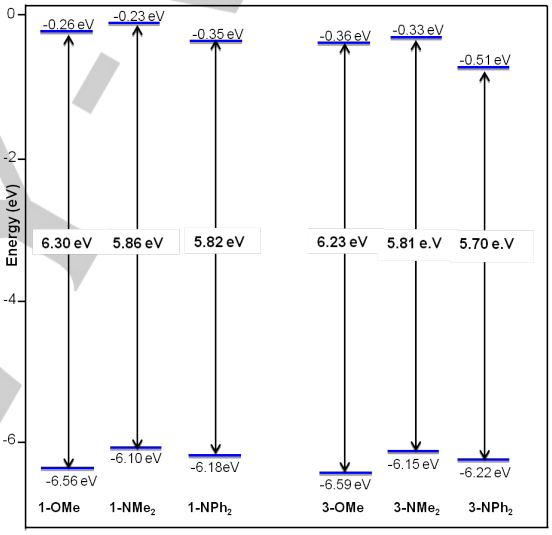

Figure 5. HOMO-LUMO gaps for **1-X** and **3-X** (X = OMe, NMe_2, NPh_2).

The TPA cross-sections (σ_2) found for the **3-X** derivatives possessing electron-releasing peripheral groups are slightly lower than those of their isocyanurate-cored analogues **1-X** (Table 2), but the relevant figures of merit reveal that the **3-X** compounds should have similar efficiencies when used in two-photon imaging applications. Our study suggests that very similar excited states are involved in the two-photon absorption process which apparently involves the lowest-energy allowed singlet state of these compounds and corresponds to the HOMO-LUMO (π*← π) transition. Replacement of the central isocyanate core by a 1,3,5-phenylene unit results in slightly lower HOMO-LUMO gaps, consistent with increased electronic coupling between the central ring and the peripheral phenyl units for the **3-X** compounds. The UV-visible spectroscopy studies have shown that the 1,3,5-phenylene ring can behave as an electron-accepting unit when coupled with strongly electron-releasing peripheral groups, in a similar fashion to the isocyanurate core. From the perturbational interpretation of NLO

phenomena,[7] this reduction in the HOMO-LUMO gap promotes 2PA at wavelengths above that of the lowest-energy absorption, which compensates for the decrease in 2PA efficiency attributable to the lower polarity of the central core in the **3-X** compounds relative to that in the **1-X** analogues. As a result, fairly similar 2PA cross-sections are found for both sets of compounds featuring electron-releasing substituents. A similar explanation rationalizes the comparable 2PA cross-sections of **1-NPh₂** and **2-NHex₂**.

As mentioned above, the slight shift to lower energy of the lowest-energy 1PA band in the **3-X** compounds and its increased intensity relative to the **1-X** analogues results in a diminished transparency window for the former. This is unfavourable for many NLO applications in the visible range,[3b] such as optical limiting at 532 nm.[18] However, the shift to lower energy of the 2PA band and the usually larger fluorescence quantum yield are beneficial for applications in the near-IR range, such as bio-imaging based on two-photon excited fluorescence.[7]

Conclusion. This work reports the linear optical properties of a series of extended 1,3,5-triphenylbenzene derivatives (**3-X**; X = NO_2, CN, H, OMe, NMe_2, NPh_2), including the synthesis and characterization of four new compounds, together with the two-photon absorption (2PA) properties of several examples (X = CN, OMe, NMe_2, NPh_2). Comparison with their known triarylisocyanurate analogues (**1-X**) reveals that the lowest-energy allowed absorption is significantly stronger, but of a similar nature ($\pi^* \leftarrow \pi$), and corresponds to a symmetrical charge transfer from the periphery of the arms toward the central ring. Except for **3-NPh₂**, the first excited state of the **3-X** compounds is more luminescent than that of the **1-X** analogues, consistent with the larger transition moment operative between the first excited state and the ground state. Despite lower HOMO-LUMO gaps, comparable or slightly lower 2PA cross-sections have been found for the **3-X** derivatives functionalized by electron-releasing substituents (OMe, NMe_2, NPh_2) relative to their **1-X** analogues, possibly because of the decreased electronegativity of the central phenylene core in the former. While their reduced transparency window makes the **3-X** compounds less attractive than their **1-X** analogues for NLO applications requiring maximal transparency in the visible range, their larger relative fluorescence quantum yields coupled to the bathochromic shift of the 2PA band and 1PA emission renders them more suited to two-photon fluorescence imaging, assuming that these properties remain unchanged folllowing functionalization for bio-compatibility.

Experimental Section

General Part. All manipulations were carried out under an inert atmosphere of argon with dried and freshly distilled solvents. Transmittance-FTIR spectra were recorded using a Perkin Elmer Spectrum 100 spectrometer equipped with a universal ATR sampling accessory (400-4000 cm^{-1}). Raman spectra of the solid samples were obtained by diffuse scattering on the same apparatus and recorded in the 100-3300 cm^{-1} range (Stokes emission) with a laser excitation source at 1064 nm (25 mW) and a quartz separator with a FRA 106 detector. High-field NMR spectroscopy experiments were performed on multinuclear Bruker 200 MHz or 400 MHz instruments (200DPX or Ascend400). Chemical shifts are given in parts per million relative to tetramethylsilane (TMS) for ^1H and ^{13}C NMR spectra. UV-Visible spectra were recorded using a Cary 5000 spectrometer or a Jasco V-570 (solutions) spectrophotometer. MS analyses were performed at the "Centre Regional de Mesures Physiques de l'Ouest" (CRMPO, Université Rennes 1) on a high-resolution MS/MS ZABSpec TOF Micromass Spectrometer. The 1,3,5-tris(4-ethynylphenyl)benzene precursor **4** was synthesized from the corresponding tris-bromophenyl precursor[2b] (see ESI). Commercial reagents were used as received.

General procedure for Sonagashira coupling reactions: 1,3,5-tris(4-ethynylphenyl)benzene (**4**; 1 eq), the appropriately functionalised halobenzene (4.5 eq), CuI (0.2 eq) and $PdCl_2(PPh_3)_2$ (0.1 eq) were dissolved in NEt_3 and either DMF or THF (1:1, 50 mL). The reaction mixture was stirred overnight at 70°C. The solvent was then removed and the dark residue purified by column chromatography on silica gel. High purity solids were obtained by recrystallisation from MeOH.

1,3,5-tris[4-(4-nitrophenyl)ethynylphenyl]benzene (3-NO₂): Following the general procedure, 1,3,5-tris(4-ethynylphenyl)benzene (**4**; 300 mg, 0.79 mmol), 4-bromonitrobenzene (721 mg, 3.57 mmol), CuI (30 mg, 0.16 mmol) and $PdCl_2(PPh_3)_2$ (56 mg, 0.08 mmol) in NEt_3/DMF, and purification by column chromatography and gradient elution DCM/hexane (1:1) to remove impurities and CH_2Cl_2/hexane (7:3) afforded the product as a yellow powder (100 mg, 17%). **Mp:** 161° (Dec.). **HRMS (EI):** m/z calcd for $C_{48}H_{27}N_3O_6$: 741.1894 $[M]^+$, found: 741.1897. **IR (KBr, $\bar{\nu}$, cm^{-1}):** 2214 (C≡C, m), 1592 (C-NO_2 *asym* & Ar, s), 1515 (Ar, s), 1342 (C-NO_2 *sym*, s). **Raman ($\bar{\nu}$, cm^{-1}):** 2213 (C≡C, s), 1605 & 1592 (C-NO_2 *asym* & Ar, s), 1343 (C-NO_2 *sym*, s), 1141 (Ar, m). **^1H NMR (500 MHz, $CDCl_3$):** δ = 8.25 (d, J = 8.9 Hz, 6H), 7.84 (s, 3H), 7.75 (d, J = 8.5 Hz, 6H), 7.73-7.67 (m, 18H). **^{13}C NMR (125 MHz, CD_2Cl_2):** δ = 147.7, 142.2, 142.1, 133.1, 133.0, 130.7, 128.0, 126.0, 124.3, 122.2, 94.9, 89.2.

1,3,5-tris-[4-(4-cyanophenyl)ethynylphenyl]benzene (3-CN): Following the general procedure, 1,3,5-tris-(4-ethynylphenyl)benzene (300 mg, 0.79 mmol), 4-iodobenzonitrile (817 mg, 3.57 mmol), CuI (30 mg, 0.16 mmol) and $PdCl_2(PPh_3)_2$ (56 mg, 0.08 mmol) in NEt_3/DMF, and purification by column chromatography, eluting with DCM/hexane (1:1), afforded the product as a yellow powder (340 mg, 63%). NMR and IR data is in agreement with literature (mp > 260 °C).[10a, 10b] **Mp:** 180° (Dec.). **Raman ($\bar{\nu}$, cm^{-1}):** 2218 (C≡C, s), 1601 (Ar, s), 1139 (Ar, m). **^1H NMR (400 MHz, $CDCl_3$):** δ = 7.82 (s, 3H), 7.73 (d, J = 8.3 Hz, 6H), 7.71-7.61 (m, 18H).

1,3,5-tris-(4-phenylethynylphenyl)benzene (3-H): Following the general procedure, 1,3,5-tris-[4-ethynylphenyl]benzene (300 mg, 0.79 mmol), 4-iodobenzene (728 mg, 3.57 mmol), CuI (30 mg, 0.16 mmol) and $PdCl_2(PPh_3)_2$ (56 mg, 0.08 mmol) in NEt_3/THF, and purification by column chromatography, eluting with CH_2Cl_2/hexane (2:3), afforded the product as a yellow powder (297 mg, 56%). **Mp:** 126° (206° Dec.). **HRMS (EI):** m/z calcd for $C_{48}H_{30}$: 607.2420 $[M+H]^+$, found: 607.2421. **IR (KBr, $\bar{\nu}$, cm^{-1}):** 2215 (C≡C, vw), 1594 (Ar, s), 1512 (Ar, s), 828 (Ar, s). **Raman ($\bar{\nu}$, cm^{-1}):** 2209 (C≡C, s), 1607 (Ar, s), 1142 (Ar, s). **^1H**

NMR (400 MHz, $CDCl_3$): δ = 7.82 (s, 3H), 7.71 (d, J = 8.4 Hz, 6H), 7.66 (d, J = 8.4 Hz, 6H), 7.59-7.55 (m, 6H), 7.41-7.34 (m, 9H). **^{13}C NMR (101 MHz, $CDCl_3$):** δ = 141.8, 140.7, 132.3, 131.8, 128.5, 128.5, 127.4, 125.2, 123.3, 122.8, 90.5, 89.4.

1,3,5-tris-[4-(4-methoxyphenyl)ethynylphenyl]benzene (3-OMe): Following the general procedure, 1,3,5-tris-(4-ethynyl-phenyl)benzene (300 mg, 0.79 mmol), 4-iodoanisole (835 mg, 3.57 mmol), CuI (30 mg, 0.16 mmol) and $PdCl_2(PPh_3)_2$ (56 mg, 0.08 mmol) in NEt_3/THF, and purification by column chromatography, eluting with ethyl acetate/hexane (3:7), afforded the product as a yellow powder (382 mg, 69%). **Mp:** 150°. **Raman ($\bar{\nu}$, cm^{-1}):** 2217 (C≡C, s), 1603 (Ar, s), 1141 (Ar, s). **^{1}H NMR (400 MHz, $CDCl_3$):** δ = 7.81 (s, 3H), 7.69 (d, J = 8.3 Hz, 6H), 7.63 (d, J = 8.2 Hz, 6H), 7.51 (d, J = 8.8 Hz, 6H), 6.90 (d, J = 8.7 Hz, 6H), 3.84 (s, 9H). **^{13}C NMR (101 MHz, $CDCl_3$):** δ = 159.8, 141.8, 140.3, 133.2, 132.1, 127.3, 125.1, 123.1, 115.4, 114.1, 90.5, 88.1, 55.4. The data are in agreement with the literature.[10c]

1,3,5-tris-[4-(4-dimethylaminophenyl)ethynylphenyl]benzene (3-NMe$_2$). Following the general procedure, 1,3,5-tris-(4-ethynyl-phenyl)benzene (300 mg, 0.79 mmol), 4-iodo-N,N-dimethylamine (881 mg, 3.57 mmol), CuI (30 mg, 0.16 mmol) and $PdCl_2(PPh_3)_2$ (56 mg, 0.08 mmol) in NEt_3/THF, and purification by column chromatography Purification by column chromatography with gradient elution from CH_2Cl_2/hexane mixtures (2:3), afforded the product as a yellow powder (268 mg, 46%). **Mp:** 175° (Dec.). **HRMS (EI):** m/z calcd for $C_{54}H_{45}N_3$: 736.3686 $[M+H]^+$, found: 736.3680. **IR (KBr, $\bar{\nu}$, cm^{-1}):** 2204 (C≡C, m), 1600 (Ar, s), 1522 (Ar, s), 814 (Ar, s). **Raman ($\bar{\nu}$, cm^{-1}):** 2208 (C≡C, m), 1601 (Ar, s), 1139 (Ar, m). **^{1}H NMR (400 MHz, $CDCl_3$):** δ = 7.80 (s, 3H), 7.68 (d, J = 8.3 Hz, 6H), 7.61 (d, J = 8.3 Hz, 6H), 7.44 (d, J = 8.8 Hz, 6H), 6.69 (d, J = 8.5 Hz, 6H), 3.01 (s, 18H). **^{13}C NMR (101 MHz, $CDCl_3$):** δ = 150.2, 141.8, 139.8, 132.9, 131.9, 127.2, 124.9, 123.6, 111.9, 110.1, 91.8, 87.5, 40.3.

1,3,5-tris-[4-(4-diphenylaminophenyl)ethynylphenyl]benzene (3-NPh$_2$): Following the general procedure, 1,3,5-tris-(4-ethynylphenyl)benzene (180 mg, 0.48 mmol), 4-iodo-N,N-diphenylaniline (795 mg 2.14 mmol), CuI (18 mg, 0.10 mmol) and $PdCl_2(PPh_3)_2$ (33 mg, 0.05 mmol) in NEt_3/THF, and purification by column chromatography, eluting with DCM/hexane (2:3), afforded the product as a yellow powder (341 mg, 65%). **Mp:** 137° (Dec.). **HRMS (EI):** m/z calcd for $C_{84}H_{57}N_3$: 1107.4547 $[M]^+$, found: 1107.4549. **IR (KBr, $\bar{\nu}$, cm^{-1}):** 2209 (C≡C, w), 1590 (Ar, s), 1515 (Ar, s), 828 (Ar, s). **Raman ($\bar{\nu}$, cm^{-1}):** 2209 (C≡C, s), 1601 (Ar, s), 1140 (Ar, s). **^{1}H NMR (500 MHz, $CDCl_3$):** δ = 7.79 (s, 3H), 7.67 (d, J = 7.8 Hz, 6H), 7.63 (d, J = 8.3 Hz, 6H), 7.42 (d, J = 8.7 Hz, 6H), 7.29 (t, J = 7.5 Hz, 12H), 7.14 (d, J = 7.3 Hz, 12H), 7.08 (t, J = 7.4 Hz, 6H), 7.04 (d, J = 8.6 Hz, 6H). **^{13}C NMR (125 MHz, $CDCl_3$):** δ = 148.1, 147.3, 141.9, 140.3, 132.7, 132.1, 129.5, 127.3, 127.3, 125.1, 123.7, 123.1, 122.4, 116.1, 90.8, 88.6.

Luminescence measurements. Luminescence measurements in solution were performed in dilute air-equilibrated solutions contained in quartz cells of 1 cm pathlength (*ca.* 10^{-6} M, optical density < 0.1) at room temperature (20 °C), using an Edinburgh Instruments (FLS920) spectrometer in photon-counting mode. Fully corrected excitation and emission spectra were obtained with an optical density at $\lambda_{exc} \leq 0.1$ to minimize internal absorption. Luminescence quantum yields were measured according to literature procedures.[19]

Two-photon excited fluorescence measurements. 2PA cross sections (σ_2) of **4-NPh$_2$** were derived from the two-photon excited fluorescence (TPEF) cross sections ($\sigma_2\Phi_F$) and the fluorescence emission quantum yield (Φ_F). TPEF cross sections were measured relative to fluorescein in 0.01 M aqueous NaOH[20] using the well-established method described by Xu and Webb[21] and the appropriate solvent-related refractive index corrections.[22] Reference values between 700 and 715 nm for fluorescein were taken from the literature.[23] The quadratic dependence of the fluorescence intensity on the excitation power was checked for each sample and at all wavelengths. A Chameleon Ultra II (Coherent) was used as excitation source, generating 140 fs pulses at 80 MHz repetition rate. The excitation was focused into the cuvette through a microscope objective (10X, NA 0.25). The fluorescence was detected in epifluorescence mode via a dichroic mirror (Chroma 675dcxru) and a barrier filter (Chroma e650sp-2p) by a compact CCD spectrometer module BWTek BTC112E. Total fluorescence intensities were obtained by integrating the corrected emission.

Computational Details. The DFT calculations reported in this work were performed using the Gaussian09 [24] program. The geometries of all the compounds were optimized without symmetry constraints using the MPW1PW91 functional[25] and the 6-31G* basis set. Solvent effects were taken into account by the Polarizable Continuum Model (PCM).[26] Calculation of the frequencies of normal modes of vibration were carried out to confirm that the optimized geometries were the true minima. TD-DFT calculations were performed at the same level of theory using the CAM-B3LYP functional[27] with the previously optimized geometries. Swizard[28] was used to plot the simulated spectra, and GausView[29] was used for the MO plots.

Acknowledgements

The CNRS (PICS program N° 7106 and LIA N° 1194) and ANR (*Isogate* Project) are acknowledged for financial support. S.S is the recipient of an Australian Postgraduate Award and thanks the Rennes Metropole for a Mobility Grant, the Australian Nanotechnology Network for an Overseas Grant, and the ANU for travel support under the Higher Degree Research Students Travel Grant Scheme. F.P. and A.N. thank the Region Bretagne for a Ph.D. grant. Mireille Blanchard-Desce ((UMR 5255, Bordeaux) is acknowledged for providing experimental facilities. M.G.H. and M.P.C. thank the Australian Research Council (ARC) for financial support. We also acknowledge the HPC resources of CINES and of IDRIS under the allocations 2016-2017[x2016080649] made by GENCI (Grand Equipement National de Calcul Intensif).

Keywords: Triphenylbenzenes • Nonlinear Optical Properties • Two-photon Absorption • Luminescence • DFT Calculations

[1] a) J. J. Wolff, R. Wortmann, *J. prakt. Chem.* **1998**, *340*, 99; b) J. Zyss, I. Ledoux, *Chem. Rev.* **1994**, *94*, 77.

[2] a) S.-H. Lee, J.-R. Park, M.-Y. Jeong, H. M. Kim, S. Li, J. Song, S. Ham, S.-J. Jeon, B. R. Cho, *Chem. Phys. Chem.* **2006**, *7*, 206; b) J. Brunel, O.

Mongin, A. Jutand, I. Ledoux, J. Zyss, M. Blanchard-Desce, *Chem. Mater.* **2003**, *15*, 4139.
[3] a) F. Terenziani, C. Katan, E. Badaeva, S. Tretiak, M. Blanchard-Desce, *Adv. Mater.* **2008**, *20*, 4541; b) G. S. He, L.-S. Tan, Q. Zheng, P. N. Prasad, *Chem. Rev.* **2008**, *108*, 1245; c) B. R. Cho, K. H. Son, S. H. Lee, Y.-S. Song, Y.-K. Lee, S.-J. Jeon, J. H. Choi, H. Lee, M. Cho, *J. Am. Chem. Chem.* **2001**, *123*, 10039; d) W. H. Lee, S. H. Lee, J.-A. Kim, J. H. Choi, M. Cho, S.-J. Jeon, B. R. Cho, *J. Am. Chem. Chem.* **2001**, *123*, 10658.
[4] D. K. Hoffmann, *J. Cell. Plast.* **1984**, *20*, 129.
[5] a) G. Argouarch, R. Veillard, T. Roisnel, A. Amar, A. Boucekkine, A. Singh, I. Ledoux, F. Paul, *New J. Chem.* **2011**, *35*, 2409; b) G. Argouarch, R. Veillard, T. Roisnel, A. Amar, H. Meghezzi, A. Boucekkine, V. Hugues, O. Mongin, M. Blanchard-Desce, F. Paul, *Chem. Eur. J.* **2012**, *18*, 11811.
[6] O. Mongin, L. Porres, C. Katan, T. Pons, J. Mertz, M. Blanchard-Desce, *Tetrahedron Lett.* **2003**, *44*, 8121.
[7] M. Pawlicki, H. A. Collins, R. G. Denning, H. L. Anderson, *Angew. Chem. Int. Ed.* **2009**, *48*, 3244.
[8] F. Paul, C. Lapinte, *Coord. Chem. Rev.* **1998**, *178/180*, 431.
[9] 1,2-alkene spacers allow usually a better electronic coupling to take place between benzene rings compared to alkyne spacers.[8]
[10] a)J . Li, A. Ambroise, S. I. Yang, J. R. Diers, J. Seth, C. R. Wack, D. F. Bocian, D. Holten, J. S. Lindsey, *J. Am. Chem. Soc.* **1999**, *121*, 8927; b) Y.-H. Kiang, G. B. Gardner, S. Lee, Z. Xu, E. B. Lobkovsky, *J. Am. Chem. Soc.* **1999**, *121*, 8204; c)E. Weber, M. Hecker, E. Koepp, W. Orlia, M. Czugler, I. Csöregh, *J. Chem. Soc., Perkin Trans. II.* **1988**, 1251.
[11] F. Paul, *work in progress*.
[12] a) E. Lippert, *Z. Natutforsch.* **1955**, *10a*, 541; b) N. Mataga, Y. Kaifu, M. Koizumi, *Bull. Chem. Soc. Jpn.* **1955**, *28*, 690.
[13] a) P. R. Bangal, D. M. K. Lam, L. A. Peteanu, M. J. Van der Auweraer, *Phys. Chem. B* **2004**, *108*, 16834; b) C. Katan, F. Terenziani, O. Mongin, M. H. V. Werts, L. Porrès, T. Pons, J. Mertz, S. Tretiak, M. Blanchard-Desce, *J. Phys. Chem. A* **2005**, *109*, 3024; c) R. Stahl, C. Lambert, C. Kaiser, R. Wortmann, R. Jakober, *Chem. Eur. J.* **2006**, 2358; d) F. Terenziani, C. Le Droumaguet, C. Katan, O. Mongin, M. Blanchard-Desce, *ChemPhysChem* **2007**, *8*, 723.
[14] H. M. Kim, B. R. Cho, *Chem. Commun.* **2009**, 153.
[15] The origin of these small deviations could be partly due to the coexistence in solution of different conformers of the species at room temperature which do not absorb at exactly the same wavelength, whereas in contrast the theoretical calculations consider only the most stable conformer.
[16] S. J. Stickler, R. A. Berg, *J. Chem. Phys.* **1962**, *37*, 814.
[17] See for instance: a) Y. Cui, S. Wang, *J. Org. Chem.* **2006**, *71*, 6485; b) W.-H. Huang, S. Wang, *Can. J. Chem.* **2006**, *84*, 477; c) J. Pang, Y. Tao, S. Freiberg, X.-P. Yang, M. D'Iorio, S. Wang, *J. Mater. Chem.* **2002**, *12*, 206.
[18] C. W. Spangler, *J. Mater. Chem.* **1999**, *9*, 2013.
[19] a) N. Demas, G. A. Crosby, *J. Phys. Chem.* **1971** *75*, 991; b) G. R. Eaton, *Pure Appl. Chem.* **1988**, *60*, 1107.
[20] M. A. Albota, C. Xu, W. W. Webb, *Appl. Opt.* **1998**, *37*, 7352.
[21] C. Xu, W. W. Webb, *J. Opt. Soc. Am. B* **1996**, *13*, 481.
[22] M. H. V. Werts, N. Nerambourg, D. Pélégry, Y. Le Grand, M. Blanchard-Desce, *Photochem. Photobiol. Sci.* **2005**, *4*, 531.
[23] C. Katan, S. Tretiak, M. H. V. Werts, A. J. Bain, R. J. Marsh, N. Leonczek, N. Nicolaou, E. Badaeva, O. Mongin, M. Blanchard-Desce, *J. Phys. Chem. B* **2007**, *111*, 9468.
[24] M. J. Frisch, G. W. Trucks, H. B. Schlegel, G. E. Scuseria, M. A. Robb, J. R. Cheeseman, G. Scalmani, V. Barone, B. Mennucci, G. A. Petersson, et al., Gaussian, Inc., Pittsburgh, PA, **2009**.
[25] C. Adamo, V. Barone, *J. Chem. Phys.* **1998**, *108*, 664.
[26] J. Tomasi, B. Mennucci, R. Cammi, *Chem. Rev.* **2005**, *105*, 2999.
[27] T. Yanai, D. P. Tew, N. C. Handy, *Chem. Phys. Lett.* **2004**, *393*, 51.
[28] S. I. Gorelsky, Revision 4.5. ed., Available from: http:// www.sg-chem.net/, University of Ottawa, Canada.
[29] R. Dennington, T. Keith, J. Millam, Semichem Inc., Shawnee Mission, KS, **2003**.

Entry for the Table of Contents

FULL PAPER

Selected optical properties of six extended triphenylbenzene derivatives are studied experimentally and theoretically (DFT). Comparison with their isocyanurate analogues reveals that in spite of the change in central spacer, nearly similar cross-sections are found for the most efficient two-photon absorbers. Possible explanations for our observations are proposed.

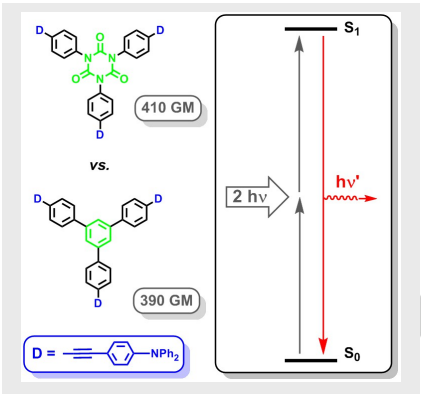

Suzy L. Streatfield, Claire Pradels, Alphonsine Ngo Ndimba, Nicolas Richy, Anissa Amar, Abdou Boucekkine, Marie P. Cifuentes, Mark G. Humphrey,* Olivier Mongin, and Frédéric Paul**

Page No. – Page No.

Electronic Absorption, Emission and Two-Photon Absorption Properties of Some Functional 1,3,5-Triphenyl-benzenes